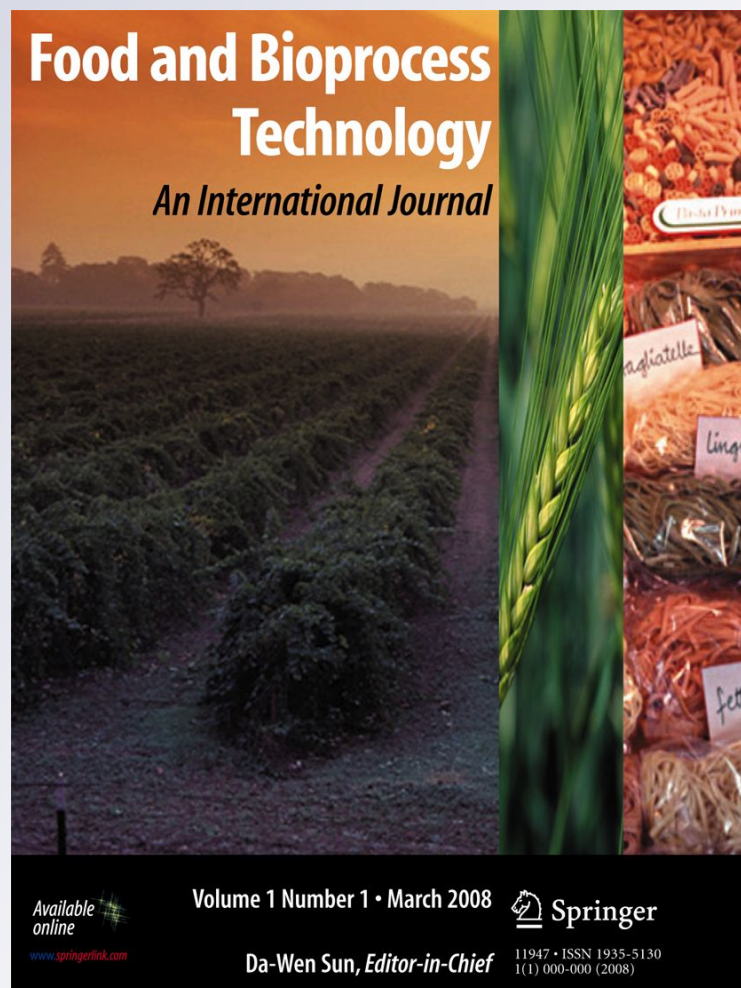# Changes in Structure, Rheology, and Water Mobility of Apple Tissue Induced by Osmotic Dehydration with Glucose or Trehalose

Sebastián Vicente, Andrea B. Nieto, Karina Hodara, María A. Castro & Stella M. Alzamora

Springer

Springer

ORIGINAL PAPER

Changes in Structure, Rheology, and Water Mobility of Apple Tissue Induced by Osmotic Dehydration with Glucose or Trehalose

Sebastián Vicente · Andrea B. Nieto · Karina Hodara · María A. Castro · Stella M. Alzamora

Abstract The impact of osmotic dehydration to water activity (a_w) at 0.97 or 0.94 with glucose or trehalose solutions on structure (optical and transmission electronic microscopy observations), rheological properties (small-scale dynamic oscillatory and creep/recovery measurements and large-scale compression force-deformation testing) and water mobility (^{1}H-NMR spectra) of parenchymatous apple tissue was investigated. In general, the nature and the concentration of sugar employed significantly affected the material properties and the structure of apple tissue. A dramatic loss in rigidity (E_d); an increase in deformation at rupture (ε_R^R), creep compliances (J_0, J_1, and J_2), and fluidity ($1/\eta_0$) and a decrease in storage (G') and loss (G'') moduli, true rupture stress (σ_R^R), and proton transverse relaxation times (T_{2i}) were induced by osmotic treatments.

ε_R^R, C_1, and T_{2i} parameters allowed to discriminate between the sugars used as osmotic agents while the different a_w levels for each sugar resulted in changes in σ_R^R, W, and T_{2i} values. Loss of turgor due to plasmolysis or rupture of membranes and desorganization/degradation of walls allowed explaining, at least partially, the changes in material parameters.

Authors Sebastián Vicente and Andrea B. Nieto share the first place.

S. Vicente · A. B. Nieto · S. M. Alzamora (✉)
Departamento de Industrias, Facultad de Ciencias Exactas y
Naturales, Universidad de Buenos Aires, Ciudad Universitaria,
1428 Buenos Aires, Argentina
e-mail: smalzamora@gmail.com

A. B. Nieto · S. M. Alzamora
Consejo Nacional de Investigaciones Científicas y Técnicas,
Buenos Aires, Argentina

K. Hodara
Departamento de Métodos Cuantitativos y Sistemas de
Información, Facultad de Agronomía,
Universidad de Buenos Aires,
Av. San Martín 4453,
C1417DSE Buenos Aires, Argentina

M. A. Castro
Departamento de Biodiversidad y Biología Experimental,
Facultad de Ciencias Exactas y Naturales,
Universidad de Buenos Aires, Ciudad Universitaria,
1428 Buenos Aires, Argentina

Introduction

Some techniques for obtaining high-moisture fruit products with characteristics close to fresh ones are based on a combination of a slight reduction of water activity (a_w), with or without previous blanching, and incorporation of antimicrobial agents and other additives to improve color and texture. Water activity depression is usually performed by osmotic dehydration in concentrated sugar aqueous solutions with simultaneous incorporation of additives achieving final values after equilibration of $a_w = 0.94$–0.97 (Alzamora et al. 1995). Mass transfer during osmotic dehydration of fruits takes place simultaneously with physical, microstructural and macrostructural modifications, loss and redistribution of water, and changes in molecular mobility, affecting strongly the material properties of plant tissues and their texture. Because of the complex connections and multivariate interdependencies, the material properties of fruit tissues are difficult to predict and to explain (Kunzek et al. 1999). Much of the past studies on osmotic dehydration of fruits have been focused on the kinetics of water/solute exchange in and out of the tissue with little evaluation of end-product quality. Contra-

dictory results exist on the effect of osmotic dehydration on material properties and texture of plant tissues, especially with respect to the nature of sugar and its concentration. The varying operative conditions used for osmotic process (at atmospheric pressure or under vacuum, dry or wet infusion, and concentration of hypertonic solution) and instrumental rheological analysis (fundamental, empirical, or imitative tests), as well as the different structure of plant tissues of distinct origin and morphology, may account for some discrepancies (Ferrando and Spiess 2001; Atarés et al. 2008; Varanyanond et al. 2001).

The relationship between some materials' properties, in particular rheological behavior, and microscopic features of plant tissues is well known. At the cellular and tissue levels, the three major structural factors that contribute to mechanical behavior of plant-based foods are turgor (i.e., the force exerted on the cell membrane by intracellular fluid), cell wall rigidity, and cell–cell adhesion, determined by the integrity of the middle lamella and the plasmodesmata (Jackman and Stanley 1995a; Waldron et al. 1997; Alzamora et al. 2000, 2008). In particular, membrane-bound water is of fundamental importance to membrane structure: hydration has been postulated to be involved in stabilizing the lipid bilayer structure within membranes and membrane-bound water may represent the rate-limiting barrier to aqueous transport (Finch and Schneider 1975). Osmotic treatment caused a redistribution of the cell membrane and a consequent reduction of the surface membrane available for swelling (Ferrando and Spiess 2001). The wall matrix is approximately composed of 75% water by mass resembling a very dense aqueous gel. Water as a solvent and lubricant significantly affects wall rheology, reducing physical interactions between wall polymers, facilitating wall creep. The hydration properties of cell wall materials are also expected to influence their rheological behavior, since suspensions of cell wall materials with a high water binding capacity form suspensions with a high yield stress, high apparent viscosity, and high elastic shear modulus (Kunzek et al. 1999).

At the macroscopic level, fruits are viscoelastic systems that exhibit a combination of elastic and viscous behavior under mechanical loading, which means that force, distance and time—in the form of rate, extent, and duration of load —determine the value of measurements (Pitt 1992). Dynamic tests provide data on viscosity and elasticity related to their time response and the dynamic mechanical spectrum appears to represent a signature of the microstructure of the material (Khan et al. 1997). Creep model parameters and G' values had also been suggested to be associated with some structural components of the fruit tissue, reflecting changes that occur at cellular level (Jackman and Stanley 1995b; Martínez et al. 2005; 2007; Alzamora et al. 2008). Various structural modifications may contribute to disassembly and loosening of primary cell walls and cell turgidity of fruits during processing, affecting creep response and storage modulus: degree of tissue turgidity, cellulose microfibrils slipping through the amorphous matrix of the wall, matrix flow, molecular regrouping of constituents (especially cellulose), or a combination of these (Alzamora et al. 2008). Knowledge resulting from investigations on plant cell structure during processing and its influence on viscoelastic behavior (determined by small deformation tests) and failure properties (determined by large deformations methods) can be utilized for the development of tailor-made technologies or the optimization of existing techniques for the production of fruits with specific mechanical properties (Kunzek et al. 1999).

Low-field nuclear magnetic resonance (NMR) has been used to non-invasively investigate the behavior and subcellular compartmentation of water in foods because of its ability to rapidly determine the mobility of water protons associated with different molecules (Micklander et al. 2002; Hills and Remigereau 1997; Ruan and Chen 2001; Thybo et al. 2004). Proton relaxation times are related to the water content of the tissue, the properties of water in different parts of the tissue, and their interaction with macromolecules and solutes, and consequently, constitute a fundamental property of the chemical and physical fruit environment (Snaar and Van As 1992; Ruan and Chen 2001). Many authors had interpreted that water exists in a number of "states" or "sites" and that these "sites" correspond to water "bound" in various ways, and relaxation times would be related to exchange between free water and various types and amounts of "bound" or "structured" water. However, Hills et al. (1990) and Hills and Duce (1990) proposed a new interpretation of proton relaxation times of water in food. They argument that such bound water undoubtelly plays a very significant role in determining the relaxation rate of water adsorbed onto biopolymers in water-poor region. But in the water-rich region (where cellular systems normally function), the contributions from chemical exchange (between water protons and exchangeable protons on the solutes and cell components) and from molecular diffusive exchange of water between the various spatial compartments comprising the tissue are expected to dominate the relaxation rate. They concluded that proton relaxation measurements in water-rich systems could give valuable information about the state of the biopolymers in the food.

Because of the need to increase our understanding about the effect of osmotic dehydration and the type of osmotic agent on material properties of apple, the main aim of the present work was to investigate the changes in the micro- and ultrastructure (by optical and transmission electronic microscopy), the rheological properties (by dynamic oscillatory shear, creep/recovery, and uniaxial compression tests), and the

state of water (by ^{1}H-NMR spectra) of apple tissues subjected to osmotic dehydration to reach a_w at 0.97 or 0.94, using glucose or trehalose as humectants. It was also explored how differences in tissue structure were expressed by viscoelastic, compression, and water mobility parameters.

Materials and Methods

Sample Preparation

Fresh apples (*Malus pumila*, Granny Smith cultivar) were obtained at similar ripening stage from a local market (86.3–88.0% moisture content, 12±1% solid content, a_w= 0.98±0.01) and stored at 5 °C. Some hours prior to use, apples were removed from refrigeration and left to equilibrate at room temperature. Each fruit was hand peeled and its core was removed. Cylinders of parenchyma tissue of 15 mm in diameter and ≥15 mm in length for compression analysis and disks of 30 mm in diameter and ≥6 mm in thickness for viscoelastic characteristics analysis were then obtained using a cork borer and a razor blade. Osmotic treatments with a_w=0.97 and 0.94 sugar solutions were carried out with apples from different batches. Fresh apple samples were used in each case as controls (called control 0.94 and control 0.97 for experiments at a_w=0.94 and 0.97, respectively).

Osmotic Dehydration

Osmotic dehydration (OD) was performed at atmospheric pressure and 20 °C by immersing the cut apples into a 22.0% (*w/w*) or 38.7% (*w/w*) glucose (glucose monohydrate, food grade, Saporiti S.A.C.I.F.I.A., Argentina) or a 34.4% (*w/w*) or 48.0% (*w/w*) trehalose (trehalose dihydrate, food grade, Cargill Inc., USA) aqueous solutions with forced convection to reach an equilibrium a_w value equal to 0.97 or 0.94, respectively. Potassium sorbate (1500 ppm, food grade, Química Oeste S.A., Argentina) and ascorbic acid (1% (*w/w*), food grade, Química Oeste S.A., Argentina) were added to the solutions and the pH was adjusted to 3.5 (natural pH of the fruit) with citric acid (0.5% (*w/w*), food grade, Química Oeste S.A., Argentina) to inhibit and/or retard microbial growth and enzymatic browning. The stirring level was chosen with the aim of making the surface mass transfer resistance negligible. A fruit-to-solution ratio 1:20 (*w/w*) was used to minimize the dilution effect on the osmotic solutions.

Sugar concentrations to obtain a_w=0.97 or 0.94 were calculated using the equation originally proposed by Norrish (1966) with correlation constant (K) equal to 2.25 for glucose and 6.47 for trehalose (Galmarini et al. 2008).

At the end of OD processes (6 to 7 h for apple disks and 18 to 20.5 h for apple cylinders), samples were taken out of the sugar solutions, rinsed in distilled water, gently dried with a tissue paper, examined for rheological and water mobility characteristics, and observed by light microscopy (LM) and transmission electron microscopy (TEM).

Measurement of Compression Properties

Mechanical behavior at large deformations was determined by uniaxial compression test with an Instron Testing Machine model 1101 (Canton, Massachusetts, USA) with a flat-end cylindrical probe of 35 mm in diameter. Compression tests were done at 10 mm/min cross-head speed and 500 N load range at ambient temperature (25 °C ±1). Each specimen was compressed between two plates to 80% deformation. From force-deformation curves (30 replicates for each condition), true stress (σ_R) (Eq. 1) and Hencky strain (ε_R) (Eq. 2) were calculated assuming constancy of sample volume during compression. Deformability modulus (E_d) was obtained from the slope of the initial linear zone of the stress–strain curve (Eq. 3). True rupture stress (σ_R^R) and true rupture strain at σ_R^R (ε_R^R) were determined from the first peak of the stress–strain curve as described by Peleg (1984). Toughness (W; i.e., the energy absorbed by the material up to the rupture point per unit of volume of the apple cylinder) was obtained by calculating the area of the stress–strain curve until the rupture point (Eq. 4) (Calzada and Peleg 1978).

$$\sigma_R = \frac{F(t).[H_0 - H(t)]}{A_0.H_0} \tag{1}$$

$$\varepsilon_R = \ln \frac{H_0}{H_0 - \Delta H} \tag{2}$$

$$E_d = \sigma_R / \varepsilon_R \tag{3}$$

$$W = \int_{\varepsilon_0}^{\varepsilon_R} \sigma \partial \varepsilon \tag{4}$$

In these equations, $F(t)$ is strength at time t, H_0 is the initial height sample, ΔH is the absolute reduction of the original height in the direction of the applied force, A_0 is the initial specimen area, $H(t)$ and H_0 are the height of the cylinder at a time of compression t and $t=0$ respectively.

Measurement of Viscoelastic Properties

Mechanical spectra and creep/recovery curves were determined at 20 °C in a Paar Physica MCR 300 controlled strain rheometer (Anton Paar GmbH, Graz, Austria) using a

30-mm diameter parallel plate head geometry with rough surface (model PP/30) and 1 N of compression to provide maximum contact area and minimum slip. Temperature was controlled by an external liquid bath thermostat model Viscotherm VT2 (Anton Paar GmbH, Graz, Austria). For both tests, data were obtained using a minimum of 11 replicates.

Dynamic oscillatory tests were performed in the controlled strain mode. To determine the linear viscoelastic range, prior to the frequency sweep, an amplitude strain sweep was carried out at an angular frequency of 10 s^{-1}. The limits of linearity were established using the US 200 software package (Paar Physica, Graz, Austria). Storage (G') and loss (G'') modules were then measured in the frequency range 0.1–100 s^{-1} using a strain amplitude value of 0.05%, within the limits of linearity previously established. The storage moduli spectra data were fitted using a linear regression:

$$\log(G') = m \log(\omega) + k \qquad (5)$$

where m is the slope and k the origin ordinate of $\log(G')$ vs. $\log(\omega)$ regression.

Creep–recovery tests were conducted by applying a constant shear stress of 35 Pa for 100 s. At this stress value, the deformation was proportional to the stress, as determined by a previous stress sweep. After removal of the stress, sample recovery was registered for an additional period of 200 s. Previously to the creep assay, the sample was subjected to two repeat loading (60 s) and unloading (120 s) cycles in order the material loss the long time memory and to remove any surface irregularity in the specimen (Mittal and Mohsenin 1987).

Compliance response was fitted with a mechanical model consisting of a spring in series with two Kelvin–Voigt elements and a dashpot element was used to fit (Sherman 1970; Jackman and Stanley 1995b) described by the following equation:

$$J(t, \tau) = (J_0) + \sum_{i=1}^{2} (J_i)\left(1 - e^{-t/\lambda_i}\right) + (t/\eta_0) \qquad (6)$$

where $J(t, \tau)$ is the creep compliance (= $\gamma(t)/\tau$ with $\gamma(t)$ being the strain at the time t and τ the constant stress applied); J_0 is the instantaneous compliance at t=0; J_i are the retarded compliances; λ_i (= $\eta_i \times J_i$) are the retardation times and η_i are the coefficients of viscosity associated with the Kelvin–Voigt elements; η_0 is the coefficient of viscosity associated with Newtonian flow and its inverse, the steady-state fluidity of the material.

Linear and nonlinear regression procedures were made using the Origin v6 (Microcal Sofware Inc., USA) software with Levenberg–Marquardt iteration method to fit the nonlinear curves.

Determination of Moisture, Soluble Solid Contents, and a_w

The weight fraction of water percent (x_w, wet basis) in apples was determined gravimetrically using a vacuum oven (Gallenkamp, United Kingdom) at 65 °C over calcium chloride as desiccant until constant weight.

Soluble solids content per cent (z_{ss}, wet basis) in the sample liquid phase was analyzed by measuring the refraction index in two refractometers (Atago, model PR 101 and model PR 200, Japan) at 25 °C.

The a_w was measured with a psycrometer (Aqua-Lab CX-2, Decagon Devices Inc., Pullman, USA) at 20 °C and calibrated with saturated aqueous solutions (Resnik et al. 1984).

Determinations were made in triplicate, and the average was reported.

Microscopic Studies

For LM of fresh and osmotically dehydrated samples, cubes of approximately 3 mm^3 taken from the central zone of the apple sample were fixed twice in 3% (w/w) glutaraldehyde solution and then in 0.1 M potassium phosphate buffer (pH 7.4) overnight at room temperature. Cubes were then rinsed three times with distilled water, postfixed in 1.5% (w/w) OsO$_4$ solution at room temperature, and dehydrated in a graded acetone series prior to being embedded in low viscosity Spurr resin (Sorrivas and Morales 1983). Sections (1–2 μm thick) of the Spurr-embedded tissue were cut on a Sorvall MT2-B ultracut microtome and stained with aqueous 1% (w/w) toluidine blue and 1% (w/w) basic fuchsin solutions and examined in a Axiscope 2 Plus light microscope (Carl Zeiss, Jena, Germany). For TEM, ultrathin sections were collected on copper grids, double stained with uranyl acetate and lead citrate (Reynolds 1963), and examined using a JEOL JEM 1200 EX II transmission electron microscope at an accelerating voltage of 80 kV.

All reagents were from Merck Química Argentina S.A. (Argentina).

Water Mobility Analysis

Transverse relaxation times (T_2) were determined at 40.0 °C in a low-resolution ^{1}H-pulsed nuclear magnetic resonance spectrometer ^{1}H-NMR Minispec PC/120 series NMR analyzer (Bruker, Karlsruhe, Germany) with an operating pulse of radio frequency radiation of 20 MHz, using the Carr–Purcell–Meiboom–Gill (CPMG) sequence with a τ value (time between 90° and 180° pulse) of 2 ms. The data

were acquired as eight scan repetitions, with a recycle delay of 4 s between each scan.

NMR relaxation signals were expressed mathematically as a sum of exponential decays according to the following equation:

$$Y = (y_0) + \sum_{i=1}^{n} (A_i)\left(e^{-t/T_{2i}}\right) \qquad (7)$$

where Y represents the NMR signal intensity at time t and n the number of uni-exponentials. The time constant associated with each uni-exponential decay or relaxation time T_{2i} corresponds to the mobility of protons in the water fraction i, and A_i reflects the apparent water content and is proportional to the number of protons in the T_{2i} state. A_i values were normalized according to the expression:

$$C_i = A_i/(A_1 + A_2 + \ldots + A_n).100$$
$$\text{with } i = 1, 2, \ldots, n \qquad (8)$$

Data were averaged over six replicates for each treatment. The Origin v6 (Microcal Sofware Inc., USA) software with Levenberg–Marquardt iteration method was used to fit the nonlinear curves. The residuals were used together with the correlation coefficient to estimate the correct number of exponential decays.

Statistical Analysis

Osmotic treatments were made using a different batch of apples for each a_w assayed, and statistics analysis was applied considering both controls.

Data from compression, creep and ^{1}H-NMR tests were analyzed by multivariate analysis of variance (MANOVA). These models compare group centroids (multivariate means of treatments) for several dependent variables jointly recorded on the same experimental units (Quinn and Keough 2002). Post hoc multiple comparisons among multivariate means of treatments were performed by Hotelling tests based on Bonferroni correction. Discriminant function analysis (DFA) was applied as an extension of multivariate analysis of variance (McGarigal et al. 2000). Previously to conduct the analyses, the assumptions of homogeneity of variance–covariance matrices and multivariate normal distribution were tested. Multivariate outliers were detected by Mahalanobis distance and removed from data set. Multicolinearity among response variables was assessed by the Pearson correlation matrix, and only uncorrelated variables were entered into the MANOVA and DFA analyses. Values of $P<0.05$ were considered to be significant in all analyses. Logarithmic transformation of data was necessary in some cases for proper use of the statistical procedure.

One-way analysis of variance (ANOVA) was applied to mechanical spectra data and significant differences among samples were determined by the Tukey's test.

Statistical analyses were carried out using InfoStat Versión 2009 (InfoStat Group, FCA-Universidad Nacional de Córdoba, Argentina).

Results and Discussion

Micro and Ultrastructure Features

LM and TEM microscopic observations allowed visualizing changes induced by the osmotic treatments at cellular level (Figs. 1 and 2). In fresh tissues, cells, rounded in shape, appeared turgid with dark walls (Fig. 1a). Turgor pressure forced the plasma membrane tightly against the cell wall. Most of the cell volume was occupied by the central vacuole and the protoplasm, bounded by the plasmalemma and the tonoplast, was present as a thin layer lining the cell surface (Figs. 1a and 2a). Some intercellular spaces with different shapes and sizes could be seen (Fig. 1a). In TEM, cell walls consisted of tightly packed and darkly stained fibrillar material and a conspicuous middle lamella in between (Fig. 2a). Fibrillar pattern was longitudinal in some zones, and clearly loose reticulate in others. Tonoplast and plasmalemma appeared intact.

Removal of water and sugar uptake clearly affected cell structure. After osmotic dehydration in 22% (w/w) glucose solution, apple tissue ($x_w=76.1$, $z_{ss}=23.4$, and $a_w=0.97$) exhibited cells clearly affected by plasmolysis with the plasma membrane detached from the wall (Fig. 1b). In many cells, membranes kept their integrity but looked collapsed, with a severe reduction of their surfaces and formation of vesicles. Walls appeared less smoothed but not collapsed. Cells were more or less regular in shape, with an arrangement similar to that of fresh fruit. This observation was in agreement with results of a previous study, where it was shown that at the beginning of osmosis in a glucose solution with the same concentration, apple tissue collapsed and cell walls folded and deformed (Nieto et al. 2004). But, at the end of the process, the cells recovered their original shape, probably due to the multicomponent diffusion process occurring during osmosis and to the relaxation of structural stresses of the compressed viscoelastic cell walls. In images acquired with TEM, cell walls in general appeared with good electron density and a notorious middle lamella (Fig. 2b). Apples tissue treated with 34.4% (w/w) trehalose solution ($x_w=62.6$, $z_{ss}=32.9$, and $a_w=0.97$) showed a slight shrinkage and increased cell-to-cell contact, reflecting their lower equilibrium moisture content compared with glucose treatment at the same a_w (Fig. 1c). The plasmalema was observed to pull away the cell wall

Fig. 1 LM micrographs of parenchyma apple tissue: **a** raw; **b** osmotically dehydrated in glucose solution, a_w=0.97; **c** osmotically dehydrated in trehalose solution, a_w=0.97; **d** osmotically dehydrated in glucose solution, a_w=0.94; **e** osmotically dehydrated in trehalose solution, a_w=0.94. *Black asterisk*, intercellular space; *black arrow*, disrupted membranes and formation of vesicles. *Scale*, 100 μm. Microphotographs **a**, **b** and **c** adapted from Ceroli 2009
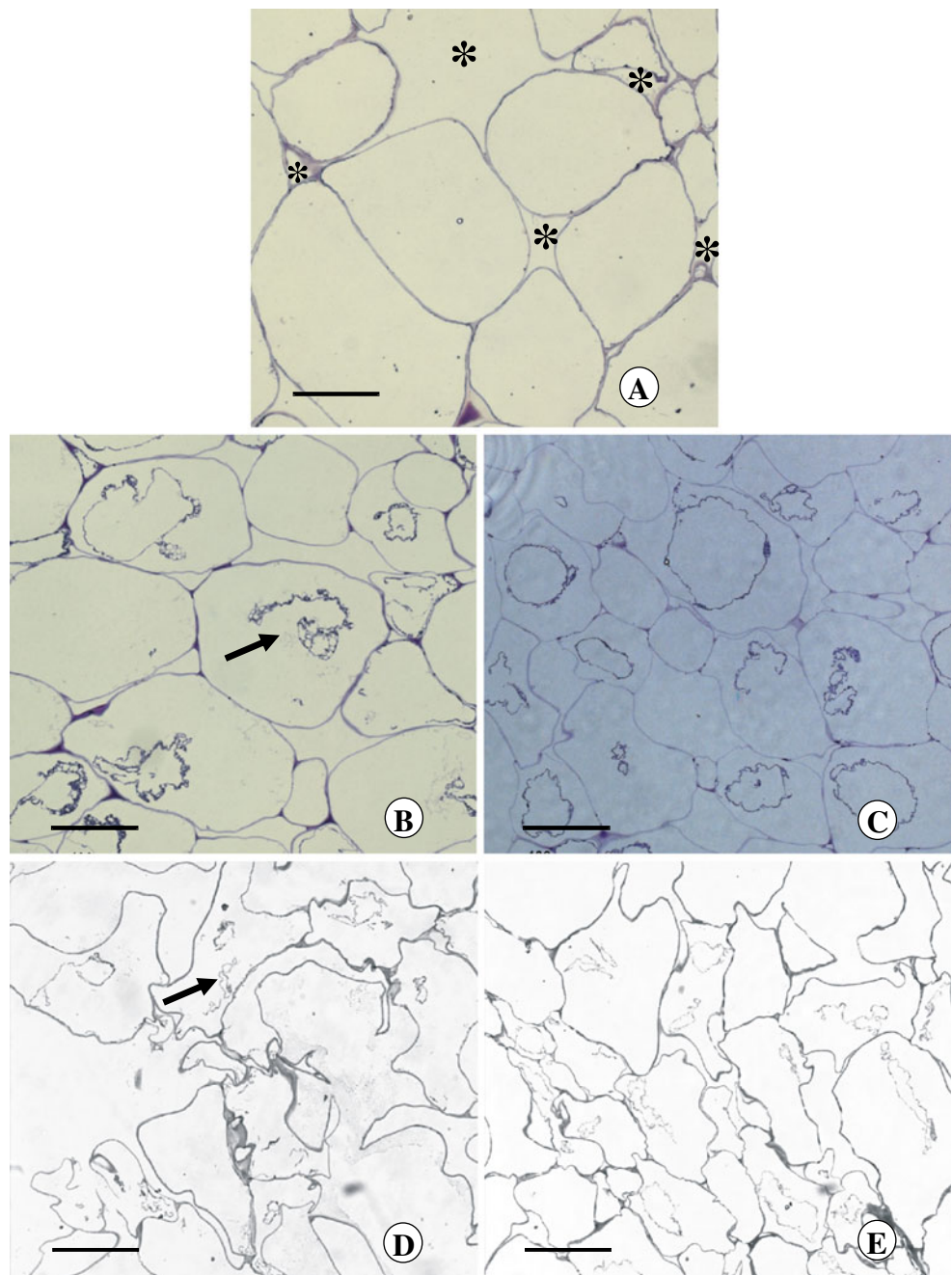

and plasmolysis was detected. Trehalose had a more protective effect on membranes than glucose: membrane integrity had been maintained in most of the cells, plasmalemma and tonoplast had not collapse, and shrunk protoplasts appeared with an unusual round shape in the center of many cells. In TEM, walls exhibited dark staining, with a clear middle lamella cementing neighboring cell walls (Fig. 2c) and a tightly fibrillar packing irregularly stained. In some images (not shown), fibrillar distribution became striated. Plasmodesmata appeared well conserved in both glucose and trehalose-treated fruits (TEM micro-

graphs not shown) and can be clearly noticed as dark punctuations in the apple walls visualized in Fig. 1b, c.

A reduction from 0.97 to 0.94 in a_w of the osmotic solutions had a dramatic effect on apple cell structure. LM and TEM images of apple tissues impregnated with glucose (x_w=50.6, z_{ss}=37.5, and a_w=0.94) or trehalose (x_w=53.7, z_{ss}=46.4, and a_w=0.94) are displayed in Figs. 1d, e and 2d–g, respectively. As a result of increased dehydration, the cells did not recover after stressing by water release and were reduced in volume (Fig. 1d, e). Plasmolysis was more severe than at a_w=0.97. In general, rupture of membranes was generalized
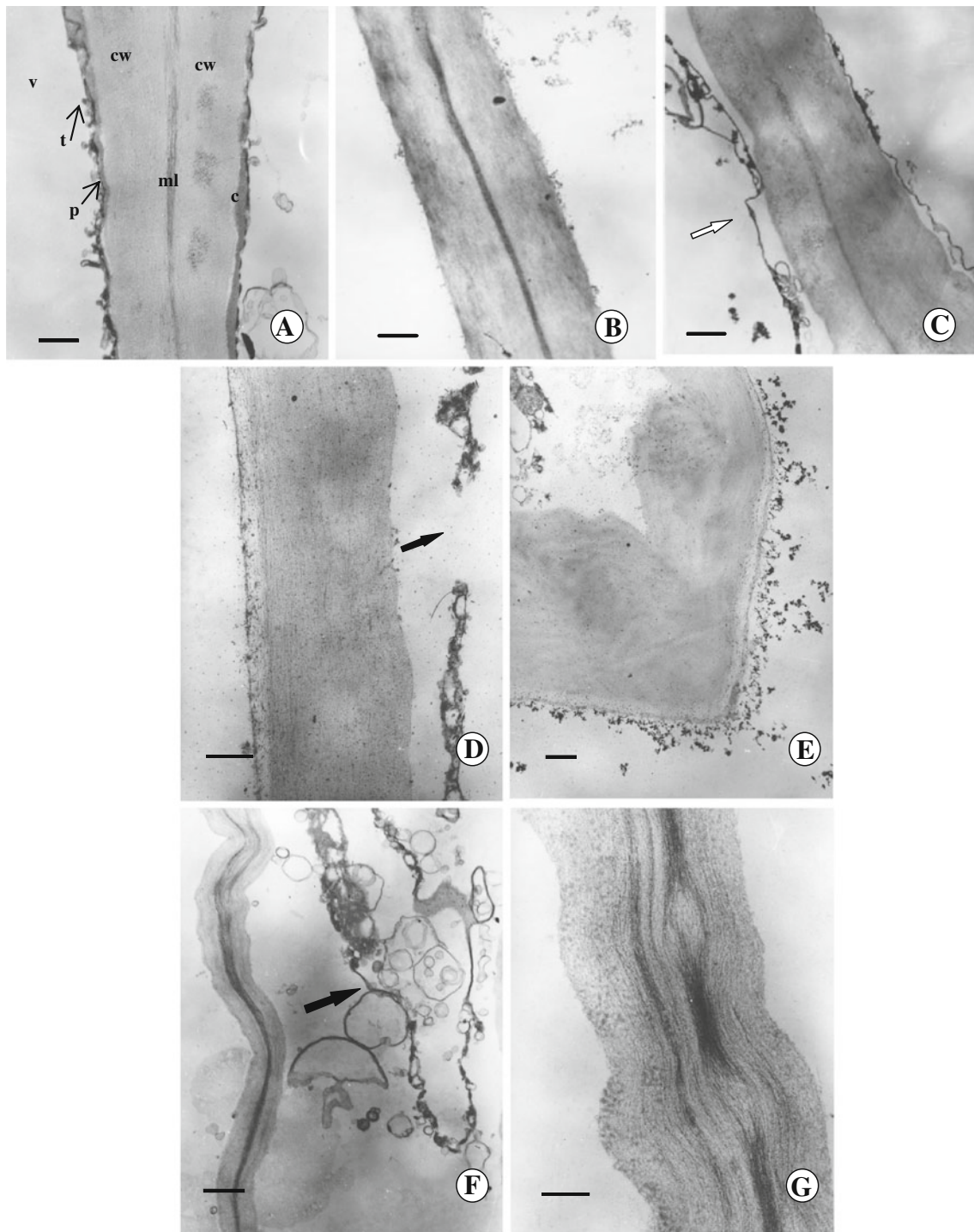
Fig. 2 TEM micrographs of parenchyma apple tissue; **a** raw; **b** osmotically dehydrated in glucose solution, a_w=0.97; **c** osmotically dehydrated in trehalose solution, a_w=0.97; **d, e** osmotically dehydrated in glucose solution, a_w=0.94. **f, g** osmotically dehydrated in trehalose solution, a_w=0.94. *White arrow*, plasmolysis; *black arrow*, disrupted membranes and formation of vesicles; *c* cytoplasm, *cw* cell wall, *ml* middle lamella, *p* plasmalemma, *t* tonoplast, *v* vacuole. *Scale*: **a, d** 500 nm; **b, c, e, f** 1 μm; **g** 200 nm

in glucose-treated tissues (Fig. 1d) while collapse of protoplast and membranes (although many of them without rupture) was detected in trehalose containing tissues (Fig. 1e). Cell walls appeared stained but much deformed and folded, with a very sinuous contour, this effect being more pronounced in treatments with trehalose solutions. As seen in TEM, fibrillar organization in glucose-treated tissue was lost, with no clearly defined pattern remaining, and the middle lamella was rarely

visualized (Fig. 2d, e). Cell wall areas containing plasmodesmata maintained their structural integrity (micrographs not shown), and this plasmodesmata-wall complexes appeared as the point of connection between the cells (dark punctuations in the walls shown in Fig. 1d). On the contrary, the middle lamella of trehalose-treated tissue appeared clearly reinforced, very well defined and thick, with a longitudinal pattern staining, denoting an specific effect of this disaccharide on wall pectin molecules (Fig. 2f, g). Tightly packed and darkly stained cellulose fibrils appeared with an intermixed pattern (Fig. 2g). Accordingly with the increase in lamellation, cells showed great contact areas cemented by the pectic substances (Fig. 1e).

The somewhat unique ability of trehalose to stabilize biomolecules, cells, and tissues during air drying is well documented (Crowe et al. 1996; Patist and Zoerb 2005; Choi et al. 2006). Trehalose (α-D-glucopyranosil-(1→1)-α-D-glucopyranoside) is a fully symmetrical disaccharide of glucose linked through an α,α-(1→1)-glycoside bond, which has more flexibility than other disaccharides to form hydrogen bonds with the biomolecules. It has been suggested that hydrogen bonding between trehalose and the polar headgroups of the lipids that constitute biomembranes contribute to preserving the integrity of biological structures (Colla et al. 2010). As the tissue is dried, these interactions replace those of hydration water at the membrane-fluid interface, maintaining the headgroups at their hydrated position and preventing the phase transition of the biomembrane from lamellar to gel phase (Patist and Zoerb 2005). Micrograph shown in Fig. 1c would confirm this mechanism. On other side, Fig. 2f, g would evidence that trehalose was participating in the network of hydrogen bonds of pectic substances. This specific effect of trehalose on walls had not yet been reported in the literature. Glucose did not show an stabilizing effect (Patist and Zoerb 2005) and accordingly membranes appeared broken and walls looked less stained, mainly at the lowest a_w (Figs. 1b, d and 2b, d, e).

Ferrando and Spiess (2001) observed a different cellular response to osmotic treatment with sucrose, maltose, and trehalose between onion epidermis and strawberry tissues: the nature of the sugar affected the shrinking behavior of onion epidermis without having any impact on the cellular shrinking of strawberry, while a protective effect of maltose and trehalose on plasmalemma was only evidenced in onion epidermis. Atarés et al. (2008) found that the kind of solute (glucose, trehalose, and sucrose) affected mass transfer during pulsed vacuum osmotic dehydration of apple, while trehalose-treated tissues rehydrated to a greater extent. Varanyanond et al. (2001) showed clear evidences for the effect of different amounts of trehalose and sucrose on the sensory texture of mango. The preferable texture, strongly correlated to adhesiveness, was attributed to the higher contents of trehalose because of the higher contribution of trehalose content to adhesiveness. Dermesonlouoglou et al. (2007) studied the effect of alternative osmotic solutes (glucose, a high DE maltodextrin, oligofructose, and trehalose) on the quality and functional properties of frozen tomato tissue. Osmodehydrofrozen compared with conventionally frozen sliced tomatoes showed improved quality and functional characteristics, with the maltodextrin and the mixture of oligofructose/trehalose before freezing causing the most desirable sensory characteristics.

Compression Behavior

Figure 3 shows notable differences in the typical true stress—true strain compression curves between fresh (control) and osmotically dehydrated apples with i_w=0.97 or 0.94. Fresh fruit exhibited an approximately linear increase of the stress with strain up to the failure point, where the stress exhibited a maximum value and then started to decline showing successive fracture events characteristic of a crisp fruit tissue. The breakdown occurred at low strain, which is the typical behavior of many fresh fruits and vegetables, such as kiwifruit and strawberries (Chiralt et al. 2001), potatoes (Luscher et al. 2005), and apples (Rebouillat and Peleg 1988; Varela et al. 2007). Osmotically dehydrated apples appeared softer and weaker than fresh apple and this effect was more pronounced for tissues with a_w=0.97, which also showed non abrupt, rounded maximum. Reduction in a_w from 0.97 to 0.94 caused a decrease in the true strain at the fracture point, an increase in rupture stress and an increase in stiffness with strain, but for both a_w values, when the osmotic agent was trehalose, the tissue resistance to deformation in response to the applied stress increased.
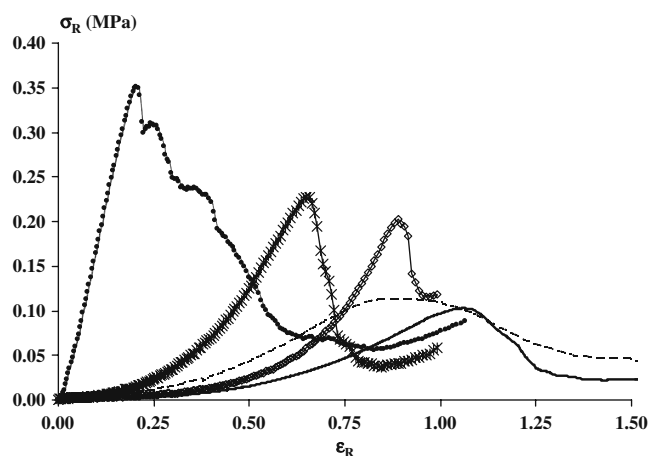
Fig. 3 Typical compression curves of true stress vs. true strain for fresh apple (control) and apples osmotically dehydrated in aqueous solutions of glucose or trehalose at a_w=0.97 or a_w=0.94. Control (circles); glucose, a_w=0.94 (error marks); glucose, a_w=0.97 (dashed line); trehalose, a_w=0.94 (diamonds); trehalose, a_w=0.97 (solid line)

Mean values of mechanical parameters (true rupture stress, σ_R^R; modulus of deformability, E_d, and deformation at the rupture point, ε_R^R) are exhibited in Table 1. Treatment group centroids were statistically different as the result of post hoc multiple comparisons (Hotelling tests, $P<0.05$) (MANOVA; treatment $F_{20,\ 652}=33.16$; $P<0.0001$; Table 1). DFA correctly classified the treatments of 93% ($n=169$) of the random apple sample test data. The first discriminant function derived from DFA accounted for most of the variation (96.59%), whereas the second discriminant function accounted for little variation (2.98%). The most important discriminating selective variables among treatments which contributed to the first discriminant function were E_d and ε_R. For the second discriminant function the most significant variable was σ_R^R. E_d values of all osmotically treated apples showed a 97–99% decrease as compared with that of untreated samples, indicating a dramatic loss in tissue rigidity induced by osmotic treatments. Only ε_R^R parameter allowed to discriminate between the sugars used as osmotic agents: apples impregnated with trehalose at any concentration showed greater ε_R^R values as compared with glucose-treated samples. The different a_w levels for both sugars resulted in changes in σ_R^R and W values: the strength and the rupture energies were higher at the lowest a_w value.

In fresh fruit tissue, the overpressure inside cells exerted by intracellular liquids on the cellular membrane and cell walls dominated the mechanics (low breaking strain and rapid crack propagation) and fracture probably occurred through the cell wall (Lillford 2001). As seen in Fig. 1, no turgor could be maintained after osmosis due to removal of water (in some cases with rupture of membranes), and consequently, osmotically treated tissues showed lower deformability modulus and increased breaking strain. Besides turgor loss, alterations in cell wall structure (redistribution of fibrils, folding of walls, potential degradation and solubilisation of macromolecules) (Fig. 2) would be the main responsible in rupture stress decrease. The greater resistance to deformation and rupture shown by tissues osmotically dehydrated to $a_w=0.94$ compared with those treated at $a_w=0.97$ could be explained by the cellular collapse and the greater solid content. Unexpectedly, the reinforcement of the middle lamella observed in $a_w=0.94$ trehalose samples did not result in an increased firmness of apple tissues.

Intercellular adhesion seemed to be maintained by the plasmodesmata structure in all osmosed tissues and also by pectic substances of the middle lamella in trehalose containing tissues and in glucose–$a_w=0.97$-treated apples. Accordingly, fracture would occur as a result of cell wall breaking instead of cell-to-cell debonding.

Viscoelastic Behavior

Figure 4 shows representative mechanical spectra of fresh and treated apples. All samples showed a viscoelastic solid behavior with the storage modulus (G') dominating the viscoelastic response. Osmotically dehydrated apple tissues with glucose or trehalose showed a pronounced decrease in G' and G'' values compared with the mechanical spectrum of untreated apple indicating that tissues became less viscous and less elastic after treatments. However, the very weak frequency linear dependence of G' for both, raw and treated tissues (m ranged from 0.06 to 0.08), corresponded to a network-type microstructure, with strongly attractive inter-particle forces and high particle concentrations (Khan et al. 1997). At low frequencies, the curves log G'' versus log ω exhibited a negative (nearly a plateau) slope while at high frequencies they showed a positive slope. The pattern found for dynamic spectra were in agreement with those previously reported for apple (Martínez et al. 2007), melon (Martínez et al. 2005), Korla pear (Wu and Guo 2010), and mashed potatoes (Alvarez et al. 2010).
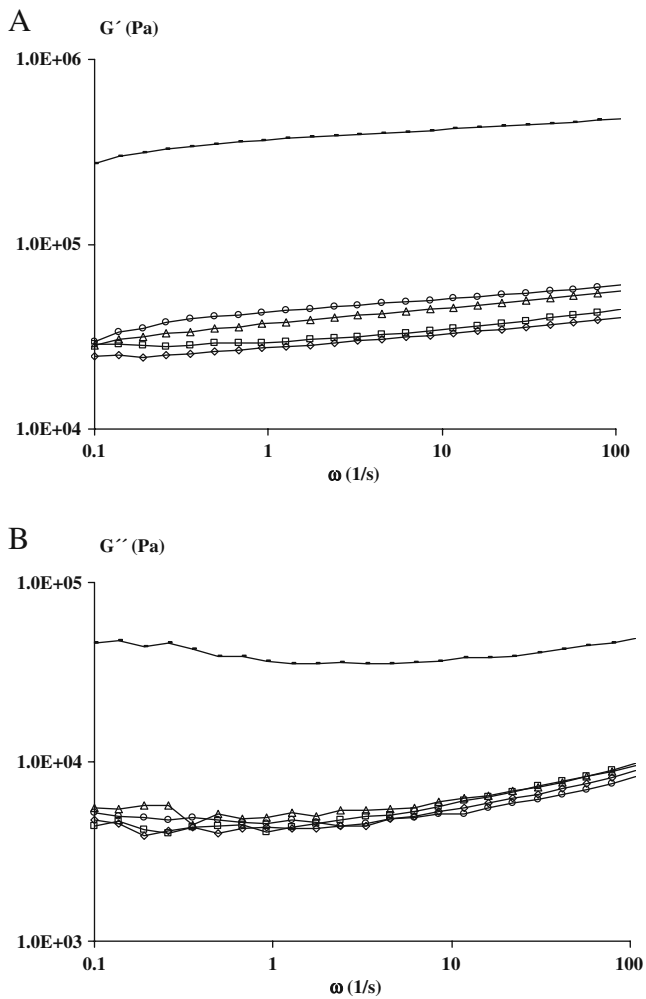
G'' and G' magnitudes were used to calculate the loss tangent values (tan $\delta=G''/G'$) (data not shown). The small differences observed in tan δ values for the different

Table 1 Mean values of compression parameters for apples osmotically dehydrated in aqueous solutions of glucose and trehalose with $a_w=0.97$ or 0.94

Treatment	σ_R^R (MPa)±SD	ε_R^R±SD	E_d (MPa)±SD	W (MJ/m³)±SD	
Control 0.97	0.33±0.04	0.26±0.02	1.7±0.2	44±8	A
Control 0.94	0.34±0.03	0.19±0.02	2.1±0.3	37±7	B
Immersed in 22.0% (w/w) glucose solution	0.11±0.02	0.79±0.06	0.04±0.01	37±6	C
Immersed in 34.4% (w/w) trehalose solution	0.12±0.02	1.02±0.07	0.02±0.01	36±5	D
Immersed in 38.7% (w/w) glucose solution	0.23±0.04	0.64±0.08	0.05±0.02	41±7	E
Immersed in 48.0% (w/w) trehalose solution	0.22±0.07	0.81±0.07	0.03±0.01	42±6	F

Post hoc multiple comparisons using Hotelling tests based on Bonferroni correction $\alpha=0.05$. Different letters indicate significant differences at $P\leq 0.05$

Control 0.97 and *Control 0.94* controls (fresh apple) for the fruit batch used for tests at $a_w=0.97$ and 0.94, respectively, *SD* standard deviation

Fig. 4 Mechanical spectrum for fresh apple (control) and apples osmotically dehydrated in aqueous solutions of glucose or trehalose at a_w=0.97 or a_w=0.94. **a** Storage modulus G′; **b** loss modulus G″. Control (*solid line*); glucose, a_w=0.97 (*circles*); glucose, a_w=0.94 (*diamonds*); trehalose, a_w=0.97 (*triangles*); trehalose, a_w=0.94 (*squares*)

is applied, and show instantaneous and complete recovery when the stress is removed. J_i parameters would be related to bonds that break and reform at different rates, the weaker bonds breaking at smaller values of time than the stronger ones. They show retarded elastic recovery. The linear region of Newtonian compliance t/η_0 would be related to those bonds that are ruptured during the shear creep step and the time required for them to reform is longer than the creep–recovery period; the released units will flow and part of the structure is not recovered (Sherman 1970). The mechanical model applied provided excellent approximation of the creep data in the time range of the experiment. It is well known that one drawback for determining creep behavior of fresh and minimal processed cut fruits is that tissue extension should be observed in short periods of time, because of the rapid change in their properties (plant tissues are usually alive, respiring and loosing water) (Alzamora et al. 2008).

Creep–recovery behavior was notoriously affected by the osmotic treatments. The MANOVA of treatments was highly significant for viscoelastic measurements ($F_{30, 265}$=5.83; $P<$0.0001), although multivariate means of 38.7% (w/w) glucose and 34.4% (w/w) and 48.0% (w/w) trehalose treatments did not differ statistically (Table 2).

The first discriminant function resulted from DFA explained 97.2% of the variance in the original variables, and the second discriminant function explained 1.8% of the remaining variance. The most important discriminating selective variables among treatments were the viscoelastic capacitances J_2 and J_1 and the retardation time λ_1 and, in a lesser degree, the instantaneous elastic capacitance J_0 and the coefficient of viscosity η_0. The 88% (n=60) of random apples were successfully classified by treatments from
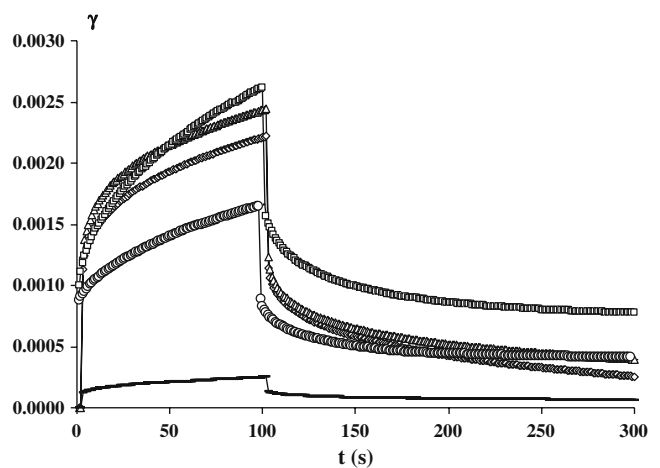
treatments (G″/G′=0.12–0.20) did not show any clear trend. ANOVA results set significant differences between control and osmotic treatments but not between the type and the concentration of sugars. Thus, mechanical spectrum analysis was not enough sensitive for distinguishing physical differences between osmotic treatments assayed.

Characteristic creep/recovery curves for fresh apples and for apples immersed in the glucose and trehalose solutions are presented in Fig. 5. The behavior of apple tissue depicted in all these curves was well characterized (correlation coefficient≥0.999) by the mechanical model represented by Eq. 6, and the corresponding parameters are supplied in Table 2. In this model, the rheological behavior of the apple tissue was defined in terms of four separate compliances. J_0 would be related to those bonds of structural units that are stretched elastically when the stress

Fig. 5 Typical experimental creep/recovery curves (deformation γ vs. time t) for fresh apples (control) and apples osmotically dehydrated in aqueous solutions of glucose or trehalose at a_w=0.97 or 0.94. Control (*solid line*); glucose, a_w=0.97 (*circles*); glucose, a_w=0.94 (*diamonds*); trehalose, a_w=0.97 (*triangles*); trehalose, a_w=0.94 (*squares*)

Table 2 Means of viscoelastic parameters derived by fitting Eq. 5 to compliance curves from creep phase for apples osmotically dehydrated in aqueous solutions of glucose and trehalose with a_w=0.97 or 0.94

Treatment	$J_0 \times 10^6$ (1/Pa)± SD	$J_1 \times 10^6$ (1/Pa)± SD	$J_2 \times 10^6$ (1/Pa)± SD	λ_1 (s)± SD	λ_2 (s)± SD	$\eta_0 \times 10^{-7}$ (Pa s) ±SD	
Control 0.94	3±1	2±1	0.9±0.3	31±15	2±1	9±2	A
Control 0.97	4±1	2.3±0.3	0.9±0.3	30±12	3±2	5±2	B
Immersed in 22.0% (w/w) glucose solution	21±2	9±2	5±1	27±7	2.8±0.4	1.05±0.06	C
Immersed in 34.4% (w/w) trehalose solution	27±3	18±3	9±3	30±7	2.7±0.4	0.6±0.1	D
Immersed in 38.7% (w/w) glucose solution	28±2	12±2	7.3±0.8	22±2	2.2±0.2	0.9±0.2	D
Immersed in 48.0% (w/w) trehalose solution	32±5	15±3	9±2	21±3	2.3±0.3	0.8±0.2	D

Post hoc multiple comparisons using Hotelling tests based on Bonferroni correction α=0.05. Different letters indicate significant differences at $P \leq$ 0.05

Control 0.97 and Control 0.94 controls (fresh apple) for the fruit lot used for tests at a_w=0.97 and 0.94, respectively, SD standard deviation

DFA. The percentage of successful prediction was perfect for glucose-treated apples at a_w=0.97 (100%), followed by control 0.97 (92% correctly classified), glucose-treated apples at a_w 0.94 (90% correctly classified), trehalose-treated apples at a_w=0.97 (89% correctly classified), control 0.94 (87% correctly classified), and trehalose-treated apples at a_w=0.94 (72% correctly classified). The corresponding DFA shows a clear separation between fresh and treated apples, which showed higher compliances (J_0, J_1, and J_2) and fluidity ($1/\eta_0$) values. Creep test results statistically differentiated the type of solute only at the highest a_w assayed. Comparison of treated samples indicated biological dissimilarities between glucose–a_w 0.97 samples (characterized by the lowest values of J_0, J_1, J_2, and $1/\eta_0$) and the rest of osmotically dehydrated apples.

All samples exhibited plastic strain which remained unrecovered in the creep/recovery test. Plasticity values (the ratio of unrecoverable or permanent deformation, t/η_0, to the total deformation, $J(t, \tau)$) of osmotically dehydrated samples were rather similar to those of untreated apples (21%, 18%, 20%, 24%, 20%, and 19% for control 0.97, control 0.94, glucose–a_w=0.97, trehalose–a_w=0.97, glucose–a_w=0.94, and trehalose–a_w=0.94-treated samples, respectively).

Cellulose (the main component of the cell wall), the turgor pressure exerted by the content of the cell on the wall and the air occluded in the matrix have been suggested as responsible of the elastic behavior of plant tissues and would influence G' values. Cellulose provides individual cells with rigidity and resistance to rupture while the turgor pressure leads to the rigidity of plant cells and tissues, and together with the cell wall, provides the mechanical support for maintaining cell and tissue shape (Carpita and Gibeaut 1993). Jackman and Stanley (1995b) proposed an interpre-

tation of a six-element creep mechanical model to analyze the multiple softening mechanisms in tomato pericarp tissue during ripening. This interpretation has been successfully used for explaining cooked potato and osmotically dehydrated melon and apple creep behavior (Alvarez et al. 1998; Martínez et al. 2005; 2007). Instantaneous elastic compliance J_0 would be related to the combination of turgor and primary cell wall strength as dictated by cellulose. Viscoelastic compliances J_1 and J_2 could be attributed to time-dependent changes in pectins and hemicelluloses respectively. Steady-state viscosity could be related to cell wall fluidity arising from exosmosis and/or solubilization and degradation of polymers and less water binding capacity due to treatments.

The removal of water provoked by osmosis, with plasmolysis of protoplasm and/or membrane breakage, contributed to turgor loss, since water contained in the vacuole determines the turgor pressure. In addition, cellulose microfibrillar patterns were disturbed. Accordingly, rigidity decreased and G' and J_0 parameter values (both influenced by the same structure elements) diminished. The change in wall characteristics and the effect of the loss of turgor would be traduced in folding and collapse of cell walls and thus in greater compliances J_1 and J_2 of treated apple samples. For apples dehydrated in glucose solutions, compliances and fluidity increased with the reduction in a_w value from 0.97 to 0.94; this behavior can be attributed to the greater degradation of cell walls at a_w=0.94 (Fig. 2d, e). J_1 and J_2 values of trehalose-treated apples were slightly greater than those of glucose-treated tissues with the same a_w; but at a_w=0.94, J_1 decreased, J_0 and $1/\eta_0$ increased, and J_2 maintained constant compared with corresponding values at a_w=0.97. These differences in the response, although not significant, could be explained by the notorious and

anomalous dark-stained wall observed in trehalose–a_w= 0.94-treated apples (Fig. 2f, g). It is to be noticed that MANOVA results did not indicate significant differences between tissues treated with trehalose at both a_w. However, this could be ascribed to the relatively large variability associated with the creep data (standard deviations), attributed to many factors, such as no homogeneity of tissues, age, sample location within the fruit, differences in intercellular space interconnectivity and cell size and aspects, etc. (Alzamora et al. 2008).

The decrease in η_0 values of treated samples indicated an increase in fluidity of the cell wall matrix. This could be attributed to the greater amount of apoplastic water due to membrane breakage (as it will be next supported by ^{1}H-NMR studies) and to solubilization and degradation of pectins and other wall biopolymers during osmosis.

Proton NMR Relaxation Time

The analysis of magnetization decay curves of fresh apple showed the presence of three components. Average values of relaxation times and relative amplitudes for control 0.97 (86.3% (w/w) moisture content) were T_{23}=950±60 ms; T_{22}=205±45 ms; T_{21}=50±11 ms; C_3=67±2%; C_2=18±4%; and C_1=15±3%. For control 0.94 (88.0% (w/w) moisture content), the mean values were T_{23}=1,207±100 ms; T_{22}=325±20 ms; T_{21}=57±8 ms; C_3=72±3%; C_2=21±2%; and C_1=17±1%. As can be observed, T_{22} and T_{23} values depended on the water content of the fresh fruit. Previous studies in fresh apples and bananas, conducted by Snaar and Van As (1992), Hills and Remigereau (1997), Hills et al. (1990), and Raffo et al. (2005), postulated that the three decay components could be ascribed to water localized in different sub-cellular components. The shortest transverse relaxation time T_{21} could distinguish water associated with cell walls, and would result of chemical exchange effect due to fast proton exchange between water and hydroxyl protons on the rigid cell wall polysaccharides (pectin, cellulose, and hemicellulose), which are characterized by low intrinsic T_2 values. The intermediate relaxation time T_{22} could be attributed to water residing in the cytoplasm and could be explained on the basis of a proton chemical exchange between water and proteins of the cytoskeleton and enzymes and the high viscosity of the cytosol. The highest relaxation time T_{23} could be assigned to water located within the vacuole. As expected, water in the vacuolar compartment had the longest relaxation times, arising from the chemical exchange with sugars and other low weight compounds that constitute the dilute solution of the sap. According to Hills and Remigereau (1997) and Hills et al. (1990), the existence of three distinct T_2 values in fresh apple meant that diffusive exchange of water between the three cell compartments was slow on the

relaxation time scale, and tonoplast and plasmalemma membranes constituted important barriers to water transport. So, each compartment exhibited a characteristic relaxation curve. Micrographs of fresh apple shown in Figs. 1 and 2 confirmed the integrity of membranes in fresh apple. Non-exchanging protons in cell wall component have proton transverse relaxation times of only a few microseconds; so they were not detectable on the millisecond timescale used in the NMR CPMG measurements.

Relaxation rates in treated apples were much faster than in fresh tissue. The transverse relaxation of water protons in osmotically dehydrated tissues was better described by two exponentials, denoting only two populations of water (Table 3). The type of osmotic treatment significantly influenced the transverse relaxation in apple cells (MANOVA; $F_{9, 126}$=23.32; P<0.0001). The first two discriminant functions explained 74.6% and 25.3% of the variance, respectively. The first contrasted T_{21} and T_{22} positively and C_1 negatively. The second axis was defined positively by T_{21} and negatively by T_{22} and C_1. DFA successfully allowed classifying the 98% of the random apple samples (n=46) by treatments. For each sugar, the relative amplitude of signals C_1 and C_2 attributed to both compartments remained substantially constant for both a_w assayed, suggesting that no marked changes in water distribution occurred with the increase in sugar concentration. On the contrary, for both sugars, T_{21} values decreased and T_{22} values increased when the concentration increased. Mean values of spin–spin relaxation times T_{21} and T_{22} groups were significantly affected by the nature of sugar used for the osmodehydration treatment: at any a_w T_{2i} values were lower in trehalose-treated tissues compared with those observed when glucose was used as osmotic agent. The trehalose ability to form a dihydrate (Patist and Zoerb

Table 3 Mean proton transverse relaxation times and signal percentages of the two components for apples osmotically dehydrated in aqueous solutions of glucose and trehalose with a_w=0.97 or 0.94

Treatment	C_1 (%)± SD	C_2 (%)± SD	T_{21} (ms)± SD	T_{22} (ms)± SD	
Immersed in 22.0% (w/w) glucose solution	24±9	76 ±9	72±25	290±38	A
Immersed in 34.4% (w/w) trehalose solution	40±8	60±9	63±12	201±20	B
Immersed in 38.7% (w/w) glucose solution	27±1	73±1	56±5	337±12	C
Immersed in 48.0% (w/w) trehalose solution	39±3	61±3	31±4	215±20	D

Post hoc multiple comparisons using Hotelling tests based on Bonferroni correction α=0.05. Different letters indicate significant differences at P≤0.05

SD standard deviation

2005), besides the higher soluble solid content of trehalose containing tissues, would result in decreased T_{2i} values.

The CPMG signals acquired from osmosed apples decayed at faster rates than those acquired from fresh apples. The major change was seen to be a reduction in the long relaxation times. One can assume that the long relaxation time corresponded to water located within the cells and the short one to water associated with the walls. At $a_w=0.97$, intrinsic relaxation time values of the protons inside cells would be reduced by the significant accumulation of soluble sugars in the space between wall and plasmalemma, the plasmolyzed cytoplasm and the vacuoles (when membranes were not broken) or inside the whole cell (in the case of broken membranes) (Cornillon 2000). But also diffusion of water molecules through field gradients because of the increased membrane permeability would contribute to relaxation time T_{22}, averaging the intrinsic relaxation times. Less mobile water molecules in the wall compartment exhibited relaxation times rather similar to those of fresh apples. Relative amplitude values C_1 and C_2 of osmosed apples compared with those of fresh fruit would suggest that some water molecules "moved" from the populations inside the cell with intermediate and high mobility to the least mobile population located in the wall, and/or that removed water mainly proceeded from vacuole and cytoplasm. The first possibility would confirm at least in part the greater fluidity ($1/\eta_0$) exhibited in the creep test by treated apples.

When the a_w of the tissue was decreased to 0.94, T_{21} values further decreased, being this effect more notable for trehalose containing tissues. Increased viscosity and proton chemical exchange could contribute to this behavior. Interestingly, the greater reduction in T_{21} of trehalose-treated tissue was in line with the notorious interaction between wall polymers and trehalose observed in Fig. 2g. In spite of the greater amount of sugars and lower water content of tissues with $a_w=0.94$ compared with tissues with $a_w=0.97$, and the smaller volumes where water could migrate (due to the contraction of the tissues), T_{22} values did not decrease and, on the contrary, they would appear to slightly increase. This could be ascribed to the release of water held in hydration layers of membranes, which undergone an important collapse or rupture, and a consequent reduction in the surface available for swelling after the osmotic treatment, as seen in Fig. 1c, d.

Conclusions

The nature of the sugar (glucose or trehalose) used as osmotic agent and the level of osmotic dehydration ($a_w=$ 0.97 or 0.94) significantly influenced compression and viscoelastic properties of apple as well as proton relaxation

and water status. A dramatic loss in tissue rigidity; an increase in deformation at rupture, creep compliances and fluidity, and a decrease in storage and loss moduli and proton transverse relaxation times were induced by osmotic treatments. $\varepsilon_R{}^R$, C_1, and T_{2i} parameters allowed to discriminate between the sugars used as osmotic agents, while the different a_w level for each sugar resulted in changes in $\sigma_R{}^R$, W, and T_{2i} values. Creep curves only differentiated the type of sugar at the lowest a_w. Many changes in material parameters could be partially explained by the alterations in the micro and ultrastructure of the tissues. Loss of turgor due to plasmolysis or rupture of membranes and desorganization/degradation of walls resulted in reduced E_d and G' modulus, increased $\varepsilon_R{}^R$ and creep compliances and decreased T_{22} at different degrees, depending on the type of solute, and the a_w value. Microscopic observations showed a specific interaction of trehalose with membranes but also with wall pectin substances at $a_w=0.94$.

This knowledge can be used to improve the osmotic process for obtaining high-moisture apples with better material properties. Further studies about the sensory impact of these osmotic agents and their concentrations are in progress.

References

Alvarez, M. D., Canet, W., Cuesta, F., & Lamua, M. (1998). Viscoelastic characterization of solids foods from creep compliance data: application to potato tissues. *Zeitschrift für Lebensmittel-Untersuchung und -Forschung A, 207,* 356–362.

Alvarez, M. D., Fernández, C., & Canet, W. (2010). Oscillatory rheological properties of fresh and frozen/thawed mashed potatoes as modified by different cryoprotectants. *Food and Bioprocess Technology, 3,* 55–70.

Alzamora, S. M., Castro, M. A., Nieto, A. B., Vidales, S. L., & Salvatori, D. M. (2000). The rol of tissue microstructure in the textural characteristics of minimally processed fruits. In S. M. Alzamora, M. S. Tapia, & A. López-Malo (Eds.), *Minimally processed fruits and vegetables* (pp. 153–171). Maryland: Aspen Publishers Inc.

Alzamora, S. M., Cerrutti, P., Guerrero, S., & López-Malo, A. (1995). Minimally processed fruits by combined methods. In G. V. Barbosa-Cánovas & J. Welti-Chanes (Eds.), *Food preservation by moisture control: fundamentals and applications* (pp. 463–492). Lancaster: Technomics Publishing Co.

Alzamora, S. M., Viollaz, P. E., Martínez, V. Y., Nieto, A. B., & Salvatori, D. M. (2008). Exploring the linear viscoelastic properties structure relationship in processed fruit tissues. In G. E. Gutiérrez-López, G. V. Barbosa-Cánovas, J. Welti-Chanes, & E. Parada-Arias (Eds.), *Food engineering: integrated approaches* (pp. 133–214). New York: Springer.

Atarés, L., Chiralt, A., & González-Martínez, C. (2008). Effect of solute on osmotic dehydration and rehydration of vacuum impregnated apple cylinders (cv. Granny Smith). *Journal of Food Engineering, 89*, 49–56.

Calzada, J. F., & Peleg, M. (1978). Mechanical interpretation of compressive stress–strain relationships of solid foods. *Journal of Food Science, 43*, 1087–1092.

Carpita, N. C., & Gibeaut, D. M. (1993). Structural models of primary cell walls in flowering plants: consistency of molecular structure with the physical properties of the walls during growth. *The Plant Journal, 3*, 1–30.

Ceroli P. (2009). *Efecto del soluto durante la dehidratación-impregnación con azúcares en las características mecánicas de tejido de manzana y de melón a altas deformaciones*. M.Sc. thesis. Argentina: Universidad de Buenos Aires.

Chiralt, A., Martínez-Navarrete, N., Martínez-Monzó, J., Talens, P., Moraga, G., Ayala, A., et al. (2001). Changes in mechanical properties throughout osmotic processes. Cryoprotectant effect. *Journal of Food Engineering, 49*, 129–135.

Choi, Y., Cho, K. W., Jeong, K., & Jung, S. (2006). Molecular dynamics simulation of trehalose as a "dynamic reducer" for solvent water molecules in the hydration cells. *Carbohydrate Research, 341*, 1020–1028.

Colla, E., Belchol Pereira, A., Hernalsteens, S., Maugeri, F., & Rodrigues, M. I. (2010). Optimization of trehalose production by *Rhodotorula dairenensis* following a sequential strategy of experimental design. *Food and Bioprocess Technology, 3*, 265–275.

Cornillon, P. (2000). Characterization of osmotic dehydrated apple by NMR and DSC. *Lebensmittel-Wissenschaft und-Technologie, 33*, 261–267.

Crowe, L. M., Reid, D. S., & Crowe, J. H. (1996). Is trehalose special for preserving dry biomaterials? *Biophysical Journal, 71*, 2087–2093.

Dermesonlouoglou, E. K., Giannakourou, M. C., & Taoukis, P. (2007). Stability of dehydrofrozen tomatoes pretreated with alternative osmotic solutes. *Journal of Food Engineering, 78*, 272–280.

Ferrando, M., & Spiess, W. E. J. (2001). Cellular response of plant tissue during the osmotic treatment with sucrose, maltose, and trehalose solutions. *Journal of Food Engineering, 49*, 115–127.

Finch, E. D., & Schneider, A. S. (1975). Mobility of water bound to biological membranas—a proton NMR relaxation study. *Biochimica et Biophysica Acta, 406*, 146–154.

Galmarini, M. V., Chirife, J., Zamora, M. C., & Perez, A. (2008). Determination and correlation of the water activity of unsaturated, supersaturated and saturated trehalose solutions. *Lebensmittel Wissenschaft und Technologie, 41*, 628–631.

Hills, B. P., & Duce, S. L. (1990). The influence of chemical and diffusive exchange on water proton transverse relaxation in plant tissues. *Magnetic Resonance Imaging, 8*, 321–331.

Hills, B. P., & Remigereau, B. (1997). NMR studies of changes in subcellular water compartmentation in parenchyma apple tissue during drying and freezing. *International Journal of Food Science and Technology, 32*, 51–61.

Hills, B. P., Takacs, S. F., & Belton, P. S. (1990). A new interpretation of proton NMR relaxation time measurements of water in food. *Food Chemistry, 37*, 95–111.

Jackman, R., & Stanley, D. (1995a). Perspectives in the textural evaluation of plant foods. *Trends in Food Science and Technology, 6*, 187–194.

Jackman, R. L., & Stanley, D. W. (1995b). Creep behaviour of tomato pericarp tissue as influenced by ambient temperature ripening and chilled storage. *Journal of Texture Studies, 26*, 537–552.

Khan, S. A., Roger, J. R. & Raghavan, S. R. (1997). Rheology: tools and methods. In: The National Academy of Sciences (ed) Aviation fuels with improved fire safety (pp 39–46) Proceedings. Washington DC, USA.

Kunzek, H., Kabbert, R., & Gloyna, D. (1999). Aspects of material science in food processing: changes in plant cell walls of fruits and vegetables. *Zeitschrift für Lebensmittel-Untersuchung und -Forschung A, 208*, 233–50.

Lillford, P. J. (2001). Mechanisms of fracture in foods. *Journal of Texture Studies, 32*, 397–417.

Luscher, C., Schlüter, O., & Knorr, D. (2005). High pressure-low temperature processing of foods: impact on cell membranes, texture, color and visual appearance of potato tissue. *Innovative Food Science & Emerging Technologies, 6*, 59–71.

Martínez, V. Y., Nieto, A. B., Castro, M. A., & Alzamora, S. M. (2007). Viscoelastic characteristics of Granny Smith apple during glucose osmotic dehydration. *Journal of Food Engineering, 83*, 394–403.

Martínez, V. Y., Nieto, A. B., Viollaz, P. E., & Alzamora, S. M. (2005). Viscoelatic behaviour of melon tissue as influenced by blanching and osmotic dehydration. *Journal of Food Science, 70*(1), 12–18.

McGarigal, K., Cushman, S., & Stafford, S. (2000). *Multivariate statistics for wildlife and ecology research*. New York: Springer.

Micklander, E., Peshlov, B., Purslow, P. P., & Engelsen, S. B. (2002). NMR-cooking: monitoring the changes in meat during cooking by low-field ^{1}H-NMR. *Trends in Food Science & Technology, 13*, 341–346.

Mittal, J. P., & Mohsenin, N. N. (1987). Rheological characterization of apple cortex. *Journal of Texture Studies, 18*, 65–93.

Nieto, A., Salvatori, D., Castro, M. A., & Alzamora, S. M. (2004). Structural changes in apple tissue during glucose and sucrose osmotic dehydration. Shrinkage, porosity, density and microscopic features. *Journal of Food Engineering, 61*(2), 269–278.

Norrish, R. S. (1966). An equation for the activity coefficient and relative humidities of water in confectionary syrup. *Journal of Food Technology, 1*, 25–28.

Patist, A., & Zoerb, H. (2005). Preservation mechanisms of trehalose in food and biosystems. *Colloids and Surfaces. B, Biointerfaces, 40*, 107–113.

Peleg, M. (1984). A note on the various strain measurements at large compressive deformations. *Journal of Texture Studies, 15*(4), 317–326.

Pitt, R. (1992). Viscoelastic properties of fruits and vegetables. In M. A. Rao & J. F. Steffe (Eds.), *Viscoelastic properties of foods* (pp. 49–76). London: Elsevier.

Quinn, G. P., & Keough, M. J. (2002). *Experimental design and data analysis for biologists*. New York: Cambridge University Press.

Raffo, A., Gianferri, R., Barbieri, R., & Brosio, E. (2005). Ripening of banana fruit monitored by wáter relaxation and diffusion ^{1}H-NMR measurements. *Food Chemistry, 89*, 149–158.

Rebouillat, S., & Peleg, M. (1988). Selected physical and mechanical properties of commercial apple cultivars. *Journal of Texture Studies, 19*, 217–230.

Resnik, S. L., Favetto, G., Chirife, J., & Ferro Fontán, C. (1984). A world survey of water activityvalues of certain saturated solutions at 25 °C. *Journal of Food Science, 49*, 510–516.

Reynolds, E. S. (1963). The use of lead citrate at high pH as an electron opaque stain in electron microscopy. *The Journal of Cell Biology, 17*, 208–212.

Ruan, R. R., & Chen, P. L. (2001). Nuclear magnetic resonance techniques. In P. Chinachoti & Y. Vodovotz (Eds.), *Bread Staling* (pp. 113–127). Boca Raton: CRC Press.

Sherman, P. (1970). *Industrial rheology*. New York: Academic.

Snaar, J. E. M., & Van As, H. (1992). Probing water compartments and membrane permeability in plant cells by ^{1}H-NMR relaxation measurements. *Biophysical Journal, 63*, 1654–1658.

Sorrivas V & Morales A (1983) Introducción a la Microscopía Electrónica. Centro Regional de Investigaciones Básicas y

Aplicadas de Bahía Blanca & Banco del Sud, Bahía Blanca, Buenos Aires, Argentina

Thybo, A. K., Karlsoon, A. H., Bertram, H. C., & Andersen, H. J. (2004). Nuclear magnetic resonance (NMR) and magnetic resonance imaging (MRI) in texture measurement. In D. Kilcast (Ed.), *Food texture: volume 2: solid foods* (pp. 184–204). Cambridge: Woodhead Publishing.

Varanyanond, W., Boonbumrung, S., Tamura, H., Yoshizawa, T., & Matsubara, Y. (2001). Osmotic dehydration of mango: influence of trehalose and sucrose contents on the product quality. *Technical Bulletin of Agriculture, Kagawa University, 53*, 43–49.

Varela, P., Salvador, A., & Fiszman, S. (2007). Changes in apple tissue with storage time: rheological, textural and microstructural analyses. *Journal of Food Engineering, 78*, 622–629.

Waldron, K. W., Smith, A. C., Parr, A. J., Ng, A., & Parker, M. L. (1997). New approaches to understanding and controlling cell separation in relation to fruit and vegetable texture. *Trends in Food Science and Technology, 8*, 213–21.

Wu, J. & Guo, K. G. (2010). Dynamic viscoelastic behavior and microstructural changes of Korla pear (*Pyrus bretschneideri rehd*) under varying turgor levels. *Biosystem Engineering*, doi:10.1016/j.biosystemseng.2010.05.014.